

1 **A statistical model for variability of the Arctic Ocean surface layer salinity**

2

3 Ekaterina Chernyavskaya¹, and Ivan Sudakov^{2,3*}

4 ¹Department of Oceanography, Arctic and Antarctic Research Institute, Bering str. 38, St.
5 Petersburg, 199397 Russia.

6 ²Department of Mathematics, University of Utah, 155 S 1400 E, Room 233, Salt Lake City, UT
7 84112-0090 USA.

8 ³Department of Informatics, Novgorod State University, B. St.-Peterburgskaya str. 41, Veliky
9 Novgorod, 173003 Russia.

10

11 * corresponding author:

12 email: sudakov@math.utah.edu

13

14 **Abstract**

15 Significant salinity anomalies were observed in the Arctic Ocean surface layer during the last
16 decade. On the base of gridded data of winter salinity of the upper 50 m layer for the period
17 1950-1993 and 2007-2012 we investigated the features of the interannual variability of salinity
18 fields, tried to identify the causes of its anomalies, and develop a statistical model for the
19 prediction of surface layer salinity fields. The Statistical model based on linear regression
20 equations linking the principal components with environmental factors such as atmospheric
21 circulation, river runoff, ice processes, and water exchange with neighboring oceans.
22 Using this model, we obtained prognostic fields of the Arctic Ocean surface layer salinity for the
23 winter period 2013-2014. Prognostic fields demonstrate the same tendencies of the surface layer
24 freshening that were observed before.

25

26 **Key words:** Arctic Basin, surface layer, salinity anomalies, empirical orthogonal functions,
27 clusters analysis.

28

29

30 **Introduction**

31 The Arctic Ocean is very sensitive to changing environmental conditions. Its surface
32 layer is a key component of the Arctic climate system, which constitutes the dynamic and
33 thermodynamic links between the atmosphere and the underlying waters (Carmack 2000). The
34 stability and development of the ice cover are associated with mixed layer thickness, upper layer
35 salinity, and upper halocline, which state the geographic distribution of sea ice and variability. In
36 this context, the Arctic Ocean surface layer is a reliable indicator of climate change in the Arctic
37 (Zaharov 1996).

38 Thermohaline structure of the Arctic Ocean surface layer has also undergone significant
39 changes in recent years (Figure 1). Of particular interest is the great freshening of the Canada
40 Basin surface layer that has not been observed in this region since 1950 (Timokhov et al. 2011)
41 until the early 1990s. However, in (Jackson et al. 2012) has emphasized that the processes
42 related to warming and freshening of the surface layer in this region have transformed the water
43 mass structure of the upper 100 m.

44 In addition, there are observations of significant salinification of the upper Eurasian Basin
45 that began around 1989. One hypothesis for this is the increasing of Arctic atmospheric cyclone
46 activity in the 1990s that led to a spectacular changing of the salinity in the Eurasian Basin. This
47 can be explained through two mechanisms of salinization: 1) changes in the rivers inflow, and 2)
48 increased brine formation due to changes in Arctic sea ice formation. The high salinization in
49 this region altered the formation of cold halocline waters, weakened vertical stratification, and
50 released heat upward from below the cold halocline layer (Johnson & Polyakov 2001). The other
51 reason of salinification is influence of the Atlantic waters (AW), which by 2007 became warmer

52 by about 0.24°C then in the 1990s. Observations show that increase in the Arctic Ocean salinity
53 has accompanied the warming. This led to significant shoaling of the upper AW boundary (up to
54 75-90 m in comparison with climatic values) and weakening of the upper-ocean stratification in
55 the Eurasian Basin as well (Polyakov et al. 2010). However, current observations also show that
56 the upper ocean of the Eurasian Basin was appreciably fresher in 2010 than it was in 2007 and
57 2008 (Timmermans et al. 2011).

58 It (Zhang et al., 2003) has been emphasized that the fresh water balance and salinification
59 of the Arctic Ocean are key players in the mixed layer. In turn, it is well known that the crucial
60 factors of the surface water mass transformation are advection of the salinized ocean waters and
61 influence of this process on the halocline and, on the other, the changes in the density field of the
62 ocean conduct to the surface water and sea ice circulation.

63 Why salinity was chosen as the object of this investigation. It is known that for the Arctic
64 Ocean, water density depends more on water salinity than on water temperature, and hence the
65 thermohaline circulation is mainly determined by salinity distribution. This conclusion comes
66 easily from an analysis of a linear equation for seawater state:

$$67 \quad \rho = \rho_0 - \varepsilon T(T - T_0) + \varepsilon S(S - S_0), \quad (1)$$

68 where ρ_0 , T_0 , S_0 are some initial values of water density, temperature, and salinity;

$$69 \quad \varepsilon T = 7 \cdot 10^{-5} \text{ g}/(\text{cm}^3 \cdot \text{K}), \quad \varepsilon S = 8 \cdot 10^{-4} \text{ g}/(\text{cm}^3 \cdot \text{‰}).$$

70 Vertical variations of temperature and salinity in the upper layer can reach 0.5°C and 1‰
71 respectively. Thus, if we put these numbers into an equation we can get the contributions of
72 temperature and salinity in changes of water density, which are about 4 and 96 % respectively.

73 Transfer of the briny surface waters and ice from the Arctic Ocean to the North Atlantic
74 is a significant component of the global ocean circulation. Thus, the investigation of the
75 variability of the surface layer can make a great contribution to understanding the climate-ocean
76 feedbacks. Particularly, abrupt changes in the surface layer salinity may lead to a tipping point in
77 the global ocean circulation (Lenton et al., 2009). In (Lenton, 2011) was defined that the climate

78 'tipping point' may happen if a small change in forcing triggers a strongly nonlinear changes of
79 the internal properties of the system, that can lead to changing its future states. We may interpret
80 a “forcing triggers” as anomaly in interannual salinity variability. Anyway, the robust
81 mathematical models are required for implementation of this hypothesis. In present time we have
82 a lot of different physical models of the surface layer salinity For example, the sea ice salinity
83 models can model significant changes in physical macroscopic properties as well as microscopic
84 properties such as the distribution of brine channels (Vancoppenolle, et al, 2009b). Besides that,
85 to use the regional climate models (for specific seas) for understanding of scale variation is not
86 an appropriate approach.

87 Thus, changes in salinification of the Arctic Ocean are one of the key players in the
88 Arctic climate system, which connects this system to the global climate system. This curious
89 system leads us to a better understanding of feedbacks, tipping points, and anomalies.

90 We propose to develop our model expressed by the ideas of L. Timokhov (Timokhov et
91 al., 2012). This statistical model of variability, of the Arctic Ocean winter salinity, in the 5–50 m
92 layer is used the method of reconstruction of the winter fields of salinity which have been
93 suggested in (Pokrovsky & Timokhov 2002). This study is devoted to the development of a
94 statistical model of variability of the Arctic Ocean winter salinity in the 5–50 m layer. The model
95 is based on equations of multiple correlations for the time series (principal components, PC)
96 associated with the first five leading modes of the Empirical Orthogonal Function (EOF) analysis
97 applied to the salinity fields. The contribution of atmospheric factors, hydrological processes and
98 pre-history of spatial distribution of salinity can be interpreted through determining of the
99 structure of the multiple correlation equations.

100 Based on gridded data of winter salinity of the upper 50 m layer for the periods of 1950-
101 1993 and 2007-2012, we investigated the features of the inter-annual variability of salinity fields,
102 tried to identify the causes of its anomalies, and made a statistical model for the prediction of
103 surface layer salinity fields.

104 Cluster analysis of the surface salinity allowed identifying 6 types of spatial distribution
105 of the salinity fields, which differ from each other by position of the fresh water core, position of
106 the Transpolar Drift frontal zone, and value of horizontal salinity gradient. It has been shown that
107 the structure of salinity fields (of 1990-1993 and 2007-2012) greatly differs from previous years.
108 Uniqueness of halin structure (during 2007-2012) was also confirmed by the results of the
109 decomposition of the surface salinity fields on Empirical Orthogonal Functions.

110 Analysis of the equations for the first five PCs showed that surface salinity fields were
111 influenced mostly by atmospheric processes. Moreover, the structure of the salinity fields due to
112 their conservatism can save and accumulate the after-effects of atmospheric processes occurring
113 up to 2-3 years ago (according to the results of the correlation analysis of the links between PCs
114 and various external factors).

115 We obtained using the PCs, calculated by the model, forecast fields of the Arctic Ocean
116 surface layer salinity for the winter period 2013-2014. Prognostic fields demonstrate the same
117 tendencies of the surface layer freshening that were observed before.

118 **2. Data Set and Method**

119 **2.1. Data Set**

120 This study is based on the collection of more than 6,419 instantaneous temperature and
121 salinity profiles with data available at the standard levels (5,10, 25, 50, 75, 100, 150, 200, 250,
122 300, 400, 500, 750, 1000 and so on every 500 meters) collected between 1950-1993 and obtained
123 from the Russian Arctic and Antarctic Research Institute (AARI) database; this is complemented
124 by data made available between 2007-2012 from the expeditions of IPY and after, which
125 consisted of CTD and XCTD data originating from ITP-buoys. The average vertical resolution of
126 these profiles were 1 m. The first database was introduced by Lebedev et al. (2008). In areas
127 where observations were missing, temperature and salinity data were reconstructed in a regular
128 grid for the period of 1950 to 1989. Also, some data was found in the joint U.S. Russian Atlas of
129 the Arctic Ocean for winter (Timokhov & Tanis 1997). Thus the working database is represented

130 by grids with spatial resolution of 200 per 200 km, covering a deep part of the Arctic Ocean
131 (with depth more than 200 m).

132 According to researchers (Treshnikov 1959; Rudels et al. 1996, 2004) the average
133 thickness of the Arctic Ocean mixed layer for the winter season is 50 m. Termohaline
134 characteristics of the surface layer fully reflect the effects of atmospheric and ice processes, as
135 water most directly exposed to the atmosphere and ice lies within the mixed layer (Sprintall &
136 Cronin 2001).

137 For data analysis, we also used different factors such as river runoff (Joint US-Russian
138 Atlas of the Arctic Ocean 1997; <http://rims.unh.edu/data/station/list.cgi?col=4>), the area of the
139 ice-free surface in the Arctic seas in September
140 (<http://www.aari.ru/projects/ECIMO/index.php?im=100>), the ice extent in the Arctic Ocean
141 (<http://www.esrl.noaa.gov/psd/data/gridded/tables/arctic.html>), and some indexes of atmospheric
142 circulation. We found AO, NAO, and PNA indexes were at <http://www.cpc.ncep.noaa.gov/>;
143 AMO indexes at <http://www.esrl.noaa.gov/psd/data/timeseries/AMO/>); and PDO data
144 downloaded from <http://jisao.washington.edu/pdo/>. Average monthly AD indexes can be found
145 at <http://www.jisao.washington.edu/analyses0302/>.

146 **2.2. The statistical method**

147 In this section, we shortly describe the statistical model for analyzing the fields of
148 oceanographic records, which was introduced in (Pokrovsky & Timokhov 2002), that was used
149 to obtain gridded salinity fields

$$150 \quad z_i = z_i^{(r)} + e, \quad \langle z_i z_j \rangle = \sigma_{x_i x_j}, \quad \langle z_i e_i \rangle = 0, \quad (2)$$
$$\langle e_i \rangle = 0, \quad \langle e_i e_j \rangle = \delta_{ij} \sigma_e^2 = \sigma_{e_{ij}}^2$$

151 We assume that $z(t, x)$ – measured value of an oceanographic record (e.g. temperature or salinity)
152 is a random function of time t and coordinates x . We can reproduce observed value of $z(t, x)$ as a
153 sum of a true value $z^{(r)}(t, x)$ of the oceanographic record and an observational error $e(t, x)$. We

154 also suppose that $z_i^{(r)}$ has spatial correlations to the records; a systematic error is not identified; a
155 standard deviation of error does exist.

156 Biorthogonal decomposition of the oceanographic record can help to identify the
157 connection between spatial and temporal distribution of the oceanographic record:

$$158 \quad z(t_j, x_i) = \sum_k c_k^j f_k(x_i) + e(t_j, x_i), \quad (3)$$

159 where $f_k(x_i)$ – spatial empirical orthogonal function (EOF); c_k^j – calculated coefficient, so-called
160 **k-th** principal component.

161 As the next step let's approximate EOF through linear combination of convenient
162 analytical functions $P_l(x_i)$. Thus, the modified biorthogonal decomposition can be written

$$163 \quad z(t_j, x_i) = \sum_k d_i^j P_l(x_i) + e(t_j, x_i), \quad (4)$$

164 here $d_i^j = \sum b_{kl} c_k^j$.

165 The main goal of this spectral analysis method is to estimate coefficients of spectral
166 decomposition $C = |c_k^j|$ and $B = \{b_{kl}\}$. Actually, this approach is a combination between singular
167 value decomposition and statistical regularization. These coefficients (modes) can be marked
168 through the real physical processes which influence salinity (see the physical model below).

169 **2.3. Statistical model**

170 Next, we will describe the approaches to data analysis which were used for physical
171 interpretation of our statistical model.

172 Researchers (Polyakov et al. 2010; Rabe et al. 2011; Morison et al. 2012) have
173 emphasized that the thermohaline structure of the surface layer has undergone significant
174 changes over the last decade. However, we still don't understand the physical processes which
175 led to these changes or what might be the future trends.

176 On the other side, we can assume that the analysis of variability of the surface layer
177 (including salinity fields) of the Arctic Ocean may be based on the decomposition of empirical
178 orthogonal function. This approach is useful in our case because decomposition on EOF gives

179 modes and principal components (PC) which allow us to divide the variability in researched
180 parameters on the spatial and temporal components. Each mode describes a certain fraction of a
181 dispersion of the initial data. This fraction is inversely proportional to the order of a mode
182 (Hannachi et al. 2007). The first 3-5 modes describe most of the dispersion of the analyzed
183 salinity fields, which allow significantly compressing the information contained in the original
184 data (Hannachi et al. 2007; Borzelli & Ligi 1998). EOF decomposition was carried out for the
185 average salinity fields for the layer 5-50 m as well as obtained time series of PCs for the periods
186 of 1950-1993 and 2007-2011.

187 We applied our statistical model to interpret the physical processes through PCs. We
188 approximate the time series of principal components to identify predictors that determine
189 variability of the salinity fields; also, it helps to obtain the equations for projection of future
190 changes. The statistical model is presented by a system of linear regression equations constructed
191 for the first five PCs, as the first five EOF yields above 77 % of the total variance of the salinity
192 data. The principal components were associated with these factors: the atmospheric circulation
193 indexes (AMO, AO, NAO, PDO, PNA, AD), water exchange with Pacific and Atlantic Oceans,
194 river runoff, and the area of the ice-free surface in the Arctic seas in September. Firstly, these
195 indexes were introduced in the work of Pokrovsky and Timokhov (2002). In table 2 you can find
196 physical interpretation of these indexes. We should note that we did introduce one assumption,
197 that time series of the Arctic and Atlantic oceans water exchange can be presented through AMO
198 indexes.

199 **2.4. Cluster analysis**

200 We use cluster analysis with the aim to systematize the existing data. You can find a
201 detailed description of cluster analysis in the work of Ward (1963). According to this approach,
202 we represent the salinity field as a grid with nodes. Each of these nodes contains information
203 about salinity in the region, and the measure of the distance between two nodes was introduced
204 through a Euclidean metric:

205
$$D_{ij} = \left(\sum_{ij} (S_i - S_j)^2 \right)^{\frac{1}{2}} \quad (5)$$

206 here S_i и S_j - value of salinity in a node for the different time.

207 Consequently, this analysis allows us to obtain the hierarchical salinity fields with a
208 feature of statistical identity (Fig.2). The figure shows that the salinity fields have structural
209 differences and thus are grouped in clusters for consecutive years. Based on the tree ties, we
210 have identified six of the largest groups in temporal scale as well as six of the basic types of
211 salinity fields. The first cluster reproduces the field for the following years - 1950-59, 1976-77
212 and 1989; the second cluster includes 1960-1965; the third cluster includes 1966-1975; the fourth
213 cluster includes 1981-1988; the fifth cluster includes 1978-1980; and the sixth cluster includes
214 1990-93 and 2007-2012 .

215 In this paper, cluster analysis was completed for the data series of an average salinity at a
216 depth of 5-25 m for the period of 1950-1989. Similar results were obtained using other methods
217 of cluster analysis (e.g., complete linkage, weighted pair-group average). This shows that the
218 chosen division into clusters is stable and proper. In addition, similar dendrograms were found in
219 the work of Koltyshev et al. (2008). It also confirms the robustness of our classification. Within
220 the framework of our classification the field type may persist for two to nine years.

221 We calculated the average salinity fields for each period of each group. It allows us to
222 find the differences (from cluster to cluster) in the structure of salinity fields (Fig.3).

223 *Cluster 1:* Our analysis for these years shows that a desalination zone occupies the
224 southern part of the Canada Basin (Fig. 3a). The salt-frontal zone lies along the Lomonosov
225 Ridge. This kind of distribution of salinity fields is formed under the dominance of a cyclonic
226 mode of the atmospheric circulation (Proshutinsky & Johnson 1997).

227 *Cluster 2:* Here the distribution of salinity fields mostly look like a freshening zone with
228 multiple cores, which extends from the Beaufort Sea to the North Pole (Fig. 3b). This structure

229 of the spatial distribution of salinity is formed because of the anticyclonic mode of the
230 atmospheric circulation at the different positions of the anticyclonic core.

231 *Cluster 3:* The main feature of the salinity distribution here is an extensive area of
232 freshening which occupies the entire Canada Basin. As a result of that, the salinity frontal zone is
233 shifted to the region of the Gakkel Ridge (Fig. 3c). This structure of the salinity spatial
234 distribution is formed at the anticyclonic mode of the atmospheric circulation.

235 *Cluster 4:* We can see here that this cluster combines the salinity fields with a tendency to
236 the formation of several zones in the prefrontal area of desalination, which is moving into the
237 area of the Gakkel Ridge (Fig. 3d).

238 *Cluster 5:* Here the core of freshening has a displacement to the region of the Makarov
239 basin to the Northeast from the slope of the Laptev Sea shelf. Freshening zone extends from
240 West to East (Fig. 3e).

241 *Cluster 6:* The zone of maximum freshening locates near to the center of the Canada
242 Basin. Also, this zone is connected to the freshening zone in the Beaufort Sea. Additionally, we
243 can see the formation of a small core of freshening close to the region which is North of the East
244 Siberian Sea. The salt-frontal zone occupies the extreme Eastern position, lying on the Makarov
245 Basin (Fig. 3f). This kind of salinity distribution is formed mainly under influence of highly
246 developed cyclonic atmospheric circulation.

247 In addition, we can note, that cluster 6 is a separate branch with the largest Euclidean
248 distance on the dendrogram. Thereby, since 1990 the structure of the salinity fields is undergoing
249 significant changes, which were most pronounced in 2007-2012. These years can be isolated in a
250 separate subbranch.

251 If we compare the variability of salinity in the Eurasian and Canada basins, we may
252 conclude that the main difference in salinity fields for 2007-2012 (included in cluster 6) is in the
253 amount of salinity of the Canada basin. During this period it was less than 0.8 ‰ comparing with

254 average values. This means there has been a significant freshening of the surface layer, which
255 has not been observed previously in more than 50 years of observation (Fig. 1).

256 **2.5. Decomposition of surface salinity fields on EOF**

257 As a result of EOF decomposition of the average salinity fields for 5-50 m layer, we
258 obtained two sets of modes and principal components for the period of 1950-1993 years (series
259 1), and for the same period by adding the 2007-2011 years (series 2). In summary, the first three
260 modes obtained by decomposition of series 1 describe over 60% of the total dispersion of the
261 initial fields; additionally, the first three modes of series 2 describe almost 67.5% of the total
262 dispersion. These modes for both decompositions are significantly different.

263 We can see that the first mode has an additional core in the Canada Basin; we observed
264 reorientation of the cores for the rest of the modes (Fig. 4). The first mode of series 1 describe
265 38% of the total salinity variability, and the first mode of series 2 takes into account 51.5% of the
266 initial data dispersion. The first mode is associated with the influence of large-scale atmospheric
267 circulation in the Arctic (Timokhov et al. 2012). Therefore, we can conclude that the role of
268 atmospheric circulation in the formation of the surface salinity fields in the Arctic Basin has
269 grown significantly over the last decade. Thus, the modes obtained by decomposition in series 1
270 cannot take into account the essential features of the distribution of surface salinity fields
271 associated with the freshening waters of the Canada Basin. Therefore, for further analysis we
272 will use the principal components and modes obtained upon decomposition of series 2.

273 Figure 5 illustrates the differences between clusters allocated previously for classification
274 of surface field salinity in terms of PCs. Clusters 1 and 6 are characterized by negative values of
275 the three principal components; the difference between the clusters is in the amount of values of
276 the principal component 1 (PC_1). Clusters 3, 4, and 5 are characterized by dominant positive
277 values PC_1 and different sign and magnitude of PC_2 and PC_3 . Cluster 5 is the opposite of cluster
278 6 in terms of PC values. As we see from Fig.3 (e, f), a shift in the signs of the principal

279 components can be explained by moving the core of freshening from the Makarov Basin to the
280 Beaufort Sea, and the degree of freshening appeared to determine the absolute value of PC₁.

281 In the late 80s, the atmospheric circulation regime began to change (Steele & Boyd 1998;
282 Kuražov et al. 2007; Proshutinsky et al. 2009; Morison et al. 2012). Degradation of the Arctic
283 anticyclone is the great example of this changing. Some changes in the structure of the surface
284 pressure field were observed. This happened because of a frequent recurrence of large values of
285 the AD indexes.

286 According to Wang et al. (2009) this could be a reason for local minima of sea ice in the
287 summers of 1995, 1999, 2002, 2005 and 2007. In addition, in the late 80s inflow of warm and
288 saline Atlantic water into the Arctic basin increased (Frolov 2009). At the beginning of this
289 century, heat flow of Pacific waters through the Bering Strait to the Chukchi Sea increased
290 (Woodgate et al. 2010).

291 We calculate a correlation of the principal components with different climate processes
292 such as the atmospheric processes, river runoff, and volume of water coming in through the
293 straits of the Arctic Basin (Table 1). Statistically significant coefficients were obtained for
294 factors reflecting influences on the processes listed above. Thus, we can assume that Cluster 6 of
295 the dendogram is the consequence of these processes.

296 The time series of some of these processes have been normalized over the interval 0 to 1.
297 We chose the clusters (1950-59, 1976-77, 1989 (cluster 1) and 1990-1993, 2007-2012 (cluster
298 6)) with a similar structure of their surface salinity fields (Fig. 3a and 3f), but with different
299 values of salinity in the water cycle of the Beaufort Sea. The histogram (Fig. 6) shows that the
300 relative values of almost all factors for the years 1990-1993 and 2007-2012 were significantly
301 higher than in the year 1950. Temperature anomalies, the area of ice-free regions of the shelf
302 seas, winter and summer AO indexes and DA indexes have reached the highest values.

303 **2.6. The linear regression equation for the principal components**

304 A set of external factors having the most correlation coefficients with the main
 305 components of salinity decomposition (Table 1) has been defined based on the results of
 306 correlation analysis. As a result of the approximation we obtained the following equations for the
 307 first five principal components:

$$\begin{aligned}
 308 \quad PC_1 = & -0.96 \times AO_{I-IV}(-2) - 1.11 \times AO_{I-IV}(-1) - 1.62 \times NAO_{XII-IV}(-1) - 3.17 \times \\
 309 \quad & AMO(-8) - 7.38 \times BS(-3) - 0.01 \times RIV_{EC}(-3) + 0.003 \times RIV_{KL}(-5) - \\
 310 \quad & 0.003 \times OW_{KLEEC}(-1) + 9.53
 \end{aligned} \tag{6}$$

$$\begin{aligned}
 311 \quad PC_2 = & -0.57 \times AO_{I-IV}(-1) - 1.49 \times AO_{VII-IX}(-1) + 6.76 \times AMO(-10) + 0.88 \times \\
 312 \quad & PDO(-3) - 0.71 \times PDO(-10) - 3.09 \times BS(-4) - 0.006 \times RIV_{LE}(-3) - 0.005 \times \\
 313 \quad & RIV_{EC}(-5) + 0.003 \times OW_{KLEEC}(-1) + 6
 \end{aligned} \tag{7}$$

$$\begin{aligned}
 314 \quad PC_3 = & -0.68 \times NAO_{XII-IV}(-3) + 7.65 \times AMO(-5) - 3.53 \times AMO(-8) - 2.42 \times \\
 315 \quad & AMO(-9) + 3.42 \times AMO(-11) + 1.40 \times PDO(-10) + 6.44 \times Tair_{II-IV}(-1) - \\
 316 \quad & 5.80 \times BS(-3) + 0.002 \times RIV_{KLEEC}(-3) - 0.002 \times RIV_{KLE}(-5) - 0.006 \times RIV_{LE}(-6) - \\
 317 \quad & 0.001 \times OW_{KLEEC}(-1) + 13
 \end{aligned} \tag{8}$$

$$\begin{aligned}
 318 \quad PC_4 = & 0.78 \times NAO_{XII-IV}(-1) + 0.59 \times PNA_{X-IV}(-1) - 0.60 \times PNA_{VII-IX}(-1) + 2.79 \times \\
 319 \quad & AMO(-6) - 2.18 \times AMO(-12) - 0.66 \times PDO(-6) - 8.27 \times BS(-4) - 0.006 \times \\
 320 \quad & RIV_{LEC}(-6) + 0.001 \times OW_{KLEEC}(-1) + 0.002 \times OW_{EC}(-1) + 8.83
 \end{aligned} \tag{9}$$

$$\begin{aligned}
 321 \quad PC_5 = & -0.68 \times NAO_{I-IV}(-1) - 2.38 \times AMO(-7) - 3.52 \times AMO(-12) + 4.72 \times \\
 322 \quad & Tair_{II-IV}(-2) + 0.001 \times IceExt(-1) - 0.002 \times RIV_{KL}(-5) + 0.007 \times RIV_{LEC}(-6) + \\
 323 \quad & 0.001 \times OW_{KLEEC}(-2) - 11.74
 \end{aligned} \tag{10}$$

324
 325
 326
 327
 328
 329 Where AO, NAO, PNA, AMO, PDO – atmospheric indices, and the lower case indicates
 330 the months of an average period; RIV – sum of annual river runoff for the arctic seas, and
 331 the lower case indicates the first letters of the sea name (K–Kara Sea, L–Laptev Sea, E–
 332 East-Siberian Sea, C–Chukchi Sea); BS – inflow through the Bering Strait; OW – sum
 333 area of open water in the arctic seas in September, and the lower case indicates the first
 334 letters of sea name; IceExt – area of ice extent in the Arctic Ocean in September; Tair –
 335 air temperature anomalies in the Arctic, and the lower case indicates months of an
 336 average period.

337 Each equation includes a set of predictors that simulate both effects of atmospheric and
 338 hydrological processes. In this case, hydrological processes have dominant influence on PC₁ (in

339 a ratio of 60/40%) and, vice versa, atmospheric processes are the major factor influencing on PC₂
340 and PC₃ in the same proportion. Atmospheric and hydrological processes make approximately
341 the same contribution (in the ratio of 47/53%) to the formation of the interannual variability of
342 PC₄.

343 **Discussion and Summary**

344 We presented here a statistical model of inter annual variability of the Arctic Ocean
345 surface layer salinity. This research builds on already established approaches used by Pokroivsky
346 and Timokhov (2002) (specifically, their reconstruction of salinity fields applying modified EOF
347 methods).

348 However, first time, our contribution to their work is the formulation of an uniform
349 statistical model, which can be used like a universal tool for analysis of inter annual variability of
350 Arctic Ocean surface layer salinity. Moreover, we suggested some additional things to improve
351 the ideas presented in previous research. For example, as opposed to this research, we do not
352 take into account the previous values of the principal components (history) that simplifies the
353 calculations and allows to increase the earliness. In addition, we also make calculations using the
354 current observational data, which is quite important for understanding the physical processes
355 during dramatic current changes in the Arctic sea ice.

356 Equations (4) - (8) describe the first five principal components for the period 1950-2014;
357 PCs for 1950-2011 obtained from these equations, have a good agreement with the values of PCs
358 directly derived from the decomposition of salinity fields on EOF (Fig. 7). Salinity fields for
359 1994-2006 can be reconstructed with the help of this model. We noted above that this period has
360 the gaps in observational data.

361 We make these conclusions because, as we mentioned in the verification, this model
362 cannot reproduce exact principle components for the short-term time series, although the trends
363 in variability of all five PC are reproduced correctly. Therefore, the model can be used for
364 tracking long-term processes of the structure transformation of salinity fields. Using this useful

365 tool we can make projections for anomalies, its frequency, and ultimately to approach an
366 understanding of these sophisticated physical processes.

367 Validation of the model was determined by calculating an error of reconstruction of
368 surface salinity fields. The difference between the real and reconstructed salinity fields is
369 determined as a percentage by the following formula:

370

$$371 \quad \text{Inc} = (\sigma(S_f - S_c) / \sigma(S_f)) \cdot 100\%, \quad (11)$$

372 where σ – standard deviation; S_f – actual salinity; S_c – calculated salinity.

373 The error in the reconstruction of salinity fields is 25.2 % (Fig. 8). The reasons for this
374 may be several:

375 1. The first five EOF modes describe more than 77 % of the variability of the initial
376 fields. It is possible that the characteristics of salinity fields may reproduce the higher order
377 modes (Borzelli & Ligi 1998). If the order of a mode increases, then the dispersion decreases.
378 So, it can enhance uncertainty in interpreting the physical processes associated to PCs. Thus, the
379 error of reconstruction in salinity fields, initially incorporated to the model, is about 23%.

380 2. Equations (6)-(10) were obtained for the continuous data series for 1950-1993.
381 However, we applied these equations to short-term and independent data series for 2007-2011.
382 Of course, it is not enough for a statistically significant assessment of the quality of PCs
383 modeling during this period. Nevertheless, the overall trend in PCs variability is reproduced
384 correctly.

385 3. In the last decade, there are significant changes in the thermohaline state of the surface
386 layer. It is quite possible that these critical transitions in this system (Timokhov et al. 2011) can
387 influence the structure of PCs. We need to adapt this model to these conditions of uncertainty.

388 Also, we apply this model for the reconstruction of salinity fields for 2013-2014. It
389 should be noted that the time series of some predictors were insufficient in length for getting
390 values of PCs. Therefore extrapolation was made.

391 As a result, we obtained the salinity field, which corresponds to the observed trends in
392 recent years. This has saved significant freshening in the Canada Basin as well as big spatial
393 gradients between the Eurasian and Canada Basins. According to our projections for 2013-2014
394 (Fig. 9), freshened water from the Beaufort Gyre will move up westward along the Siberian
395 continental slope. In 2014, the spatial structure of the salinity field is similar to the structure that
396 is typical for fields belonging to cluster 4 (1981-1988), but they differ by the surface salinity
397 values in the Beaufort Sea.

398

399 **Acknowledgments**

400 In preparing this text, we have benefited from discussions with L.A. Timokhov and Jessica R.
401 Houf. We are grateful for the financial support from Otto Schmidt Laboratory for Polar and
402 Marine Research (grant No. OSL-13-05) and from Russian Foundation for Basic Research (grant
403 No. 14-01-31053 мол_a). IS acknowledges support from “Mathematics and Climate Research
404 Network” (NSF-funded project, grant No. DMS-0940249) and from the Russian Federation
405 President Grant (No. MK-128.2014.1). IS acknowledges the kind hospitality of the Isaac Newton
406 Institute for Mathematical Sciences (Cambridge, UK) and of the Mathematics for the Fluid Earth
407 2013 programme, as well as the Dynasty Foundation for their support.

408

409 **References:**

- 410 Borzelli G. & Ligi R. 1998. Empirical Orthogonal Function Analysis of SST Image Series: a
411 Physical Interpretation. *Journal of atmospheric and oceanic technology*, vol. 16, p. 682-
412 690.
- 413 Carmack E.C. 2000: The Arctic Ocean’s freshwater budget: sources, storage and export. In E.L.
414 Lewis, E.P. Jones, P. Lemke, T.D. Prowse, P. Wadhams (eds.): *The Freshwater Budget*
415 *of the Arctic Ocean*. Pp.91-126. Netherlands: Kluwer Academic Publishers.

- 416 Chernyavskaya E.A., Timokhov L.A. & Nikiforov E.G. 2013. Karakteristiki poverhnostnogo
417 sloja i podstilajušćego ego haloklina Arctičeskogo bassejna v zimnij period (po dannym
418 1973-1979 gg). (Characteristics of the Arctic Ocean surface layer and underlying
419 halocline in winter (according to the 1973-1979 period)). *Problemy Arktiki i Antarktiki*
420 1(95), p. 5-17.
- 421 Hannachi A., Jolliffe I.T. & Stephenson D.B. 2007. Empirical orthogonal functions and related
422 techniques in atmospheric science: a review. *International Journal of Climatology* 27,
423 1119-1152.
- 424 Morison J. et al. 2012. Changing Arctic Ocean freshwater pathways. *Nature* 481, 66-70, doi
425 10.1038/nature10705
- 426 Overland J. E. & Wang M. 2007. Future regional sea ice declines. *Geophysical Research Letters*
427 34, L17705, doi 10.1029/2007GL030808.
- 428 Overland J. E., Wang M. & Salo S. 2008. The recent Arctic warm period. *Tellus* 60A, p.589-597.
- 429 Overland J.E. & Wang M. 2010. Large-scale atmospheric circulation changes are associated with
430 the recent loss of Arctic sea ice. *Tellus* 62A, p.1-9.
- 431 Pokrovsky O.M. & Timokhov L.A. 2002. Rekonstrukcyja zimnih polej temperatury i solenosti
432 Severnogo Ledovitogo okeana (The Reconstruction of the Winter Fields of the Water
433 Temperature and Salinity in the Arctic Ocean). *Okeanologija*, vol.42, №6, p. 822-830.
- 434 Polykov I. V. et al. 2010. Arctic Ocean warming contributes to reduced Polar Ice Cap. *Journal of*
435 *Physical Oceanography*, vol. 40, p. 2743-2756
- 436 Proshutinsky A.Y. & Johnson M.A. 1997. Two circulation regimes of the wind-driven Arctic
437 Ocean. *Journal of Geophysical Research*, vol. 102, № C6, p. 12493-12514.
- 438 Proshutinsky A.Y. et al. 2009. Beaufort Gyre freshwater reservoir: State and variability from
439 observations. *Journal of Geophysical Research*, vol. 114, doi 10.1029/2008JC005104
- 440 Rabe B. et al. 2011. An assessment of Arctic Ocean freshwater content changes from the 1990s
441 to the 2006-2008 period. *Deep-Sea Research* 58, p. 173-185.

- 442 Rudels B., Anderson L.G. & Jones E.P. 1996. Formation and evolution of the surface mixed
443 layer and halocline of the Arctic Ocean. *Journal of Geophysical Research*, vol. 101,
444 №C4, p. 8807-8821.
- 445 Rudels B. et al. 2004. Atlantic sources of the Arctic Ocean surface and halocline waters. *Polar*
446 *Research*, vol. 23, №4, p. 181-208.
- 447 Sprintall J. & Cronin M. F. 2001. Upper ocean vertical structure. *Encyclopedia of ocean sciences*
448 6, p. 3120-3129.
- 449 Steele M. & Boyd T. 1998. Retreat of the cold halocline layer in the Arctic Ocean. *Journal of*
450 *Geophysical Research*, vol. 103, doi 10.1029/98JC00580
- 451 Stroeve J. et al. 2007. Arctic sea ice decline: Faster than forecast. *Geophysical Research Letters*
452 34, L09501, doi 10.1029/2007GL029703
- 453 Timmermans M.-L. et al. 2011. Surface freshening in the Arctic Ocean's Eurasian Basin: an
454 apparent consequence of recent change in the wind-driven circulation. *European*
455 *Geosciences Union General Assembly 2011. Austria, Vienna, 3-8 April 2011.*
456 *Geophysical Research Abstracts 13*, EGU2011-5190.
- 457 Timokhov L. & Tanis F. (eds.) 1997. *Joint U.S.-Russian Atlas of the Arctic Ocean [CD-ROM].*
458 *Environmental Working Group*. Boulder, USA: University of Colorado.
- 459 Timokhov L.A. et al. 2011: Èkstremaal'nye izmenenija temperatury i solenosti vody arctičeskogo
460 poverhnostnogo sloja v 2007-2009 gg. (The extreme changes of temperature and salinity
461 in the Arctic Ocean surface layer in 2007-2009.) In I.Y. Frolov (ed.): *Okeanografija i*
462 *morskoj led. (Oceanography and sea ice.)* Pp.118-137. Moscow: Paulsen.
- 463 Timokhov L.A. et al. 2012. Statističeskaja model' mežgodovoj izmenčivosti polej zimnej
464 solenosti poverhnostnogo sloja. (Statistical model of interannual variability of the Arctic
465 Ocean surface layer salinity in winter). *Problemy Arktiki i Antarktiki*, 1(91), p. 89-102.
- 466 Trešnikov A.F. 1959. Poverhnostnye vody v Arctičeskom bassejne. (Arctic Ocean surface
467 waters.) *Problemy Arktiki* 7, p. 5-14.

468 Wang J. et al. 2009. Is the Dipole Anomaly a major driver to record lows in Arctic summer sea
469 ice extent? *Geophysical Research Letters* 36, L05706, doi 10.1029/08GL036706

470 Ward J.H. 1963. Hierarchical Grouping to Optimize an Objective Function. [Journal of the](#)
471 [American Statistical Association](#) 58, p. 236-244.

472 Woodgate R.A., Weingartner T. & Lindsay R. 2010. The 2007 Bering Strait oceanic heat flux
473 and anomalous Arctic sea-ice retreat. *Geophysical Research Letters* 37, L01602, doi
474 10.1029/2009GL041621

475 Wu B., Wang J. & Walsh J.E. 2006. Dipole Anomaly in the Winter Arctic Atmosphere and Its
476 Association with Sea Ice Motion. *Journal of Climate*, 19, p. 210–225.

477 Zaharov V.F. 1996. *Morskie l'dy v klimatičeskoj sisteme. (Sea ice in the climatic system)*. Saint-
478 Petersburg: Hydrometeoizdat (Gidrometeoizdat).

479 Koltyšev A.E. et al. 2008. Krupnomasštabnaja izmenčivost' arealov rasprostraneniya
480 raspresnennyh vod v Arktičeskom bassejne. (Large-scale variability of areas of the Arctic
481 Ocean fresh water distribution.). *Trudy AANII* 448, p. 37–58.

482 Lebedev N.V. et al. 2008. Specializirovannaja baza dannyh po temperature i solenosti vod
483 Arktičeskogo bassejna i okrainnyh morej v zimnij period. (Specialized database for
484 temperature and salinity of the Arctic Basin and marginal seas in winter.) *Trudy AANII*
485 448, p. 5-17.

486 Frolov I.E. et al. 2005. *Naučnye issledovanija v Arktike. (Scientific researches in Arctic.)* Vol. 1.
487 Saint-Petersburg: Nauka.

488 Zhang, Xiangdong, Moto Ikeda, John E. Walsh, 2003: Arctic Sea Ice and Freshwater Changes
489 Driven by the Atmospheric Leading Mode in a Coupled Sea Ice–Ocean Model. *J.*
490 *Climate*, 16, 2159–2177. doi: <http://dx.doi.org/10.1175/2758.1>

491 T.M. Lenton, H. Held, E. Kriegler, J. W. Hall, W. Lucht, S. Rahmstorf, and H. J. Schellnhuber,
492 Tipping elements in the Earth's climate system, *Proceedings of the National Academy of*
493 *Sciences* 105 (2008), 1786-1793.

494 Lenton, T.M. (2011). Early warning of climate tipping points. *Nature Climate Change*, 1, 201-
495 209.

496 Pokrovsky O.M., L.A. Timokhov., The reconstruction of the winter fields of the temperature and
497 salinity in the Arctic ocean, *Okeanologiya (Oceanology)*, 42(6), p. 822830.

498 Jackson, J. M., W. J. Williams, and E. C. Carmack (2012), Winter sea-ice melt in the Canada
499 Basin, Arctic Ocean, *Geophys. Res. Lett.*, 39, L03603, doi:10.1029/2011GL050219.

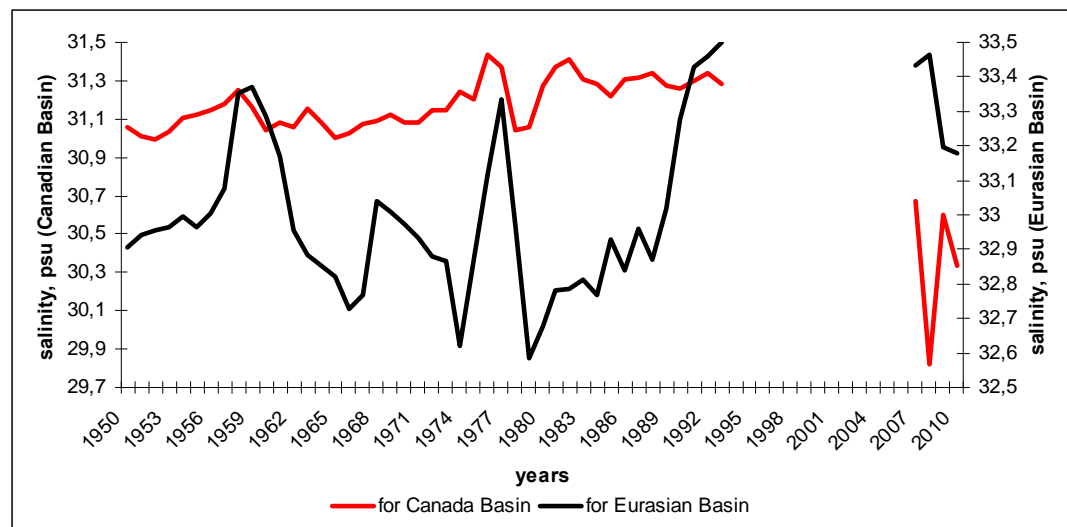
500 Vancoppenolle, M., T. Fichefet, and H. Goosse (2009b). Simulating the mass balance and
501 salinity of Arctic and Antarctic sea ice. 2. Importance of sea ice salinity variations, *Ocean*
502 *Modelling*, 27, 54-69

503

504

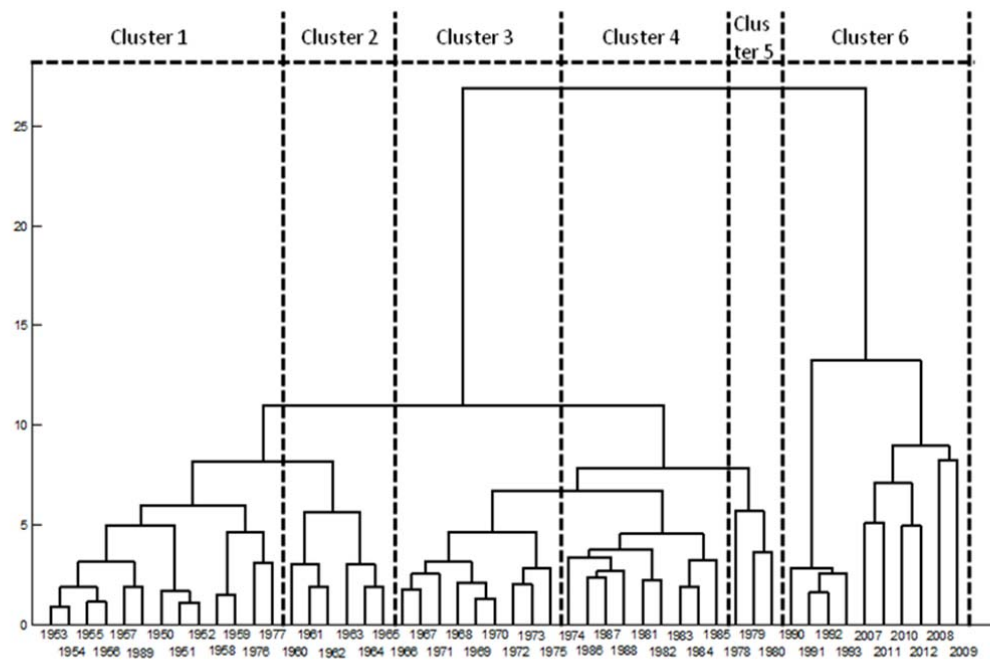
505

506



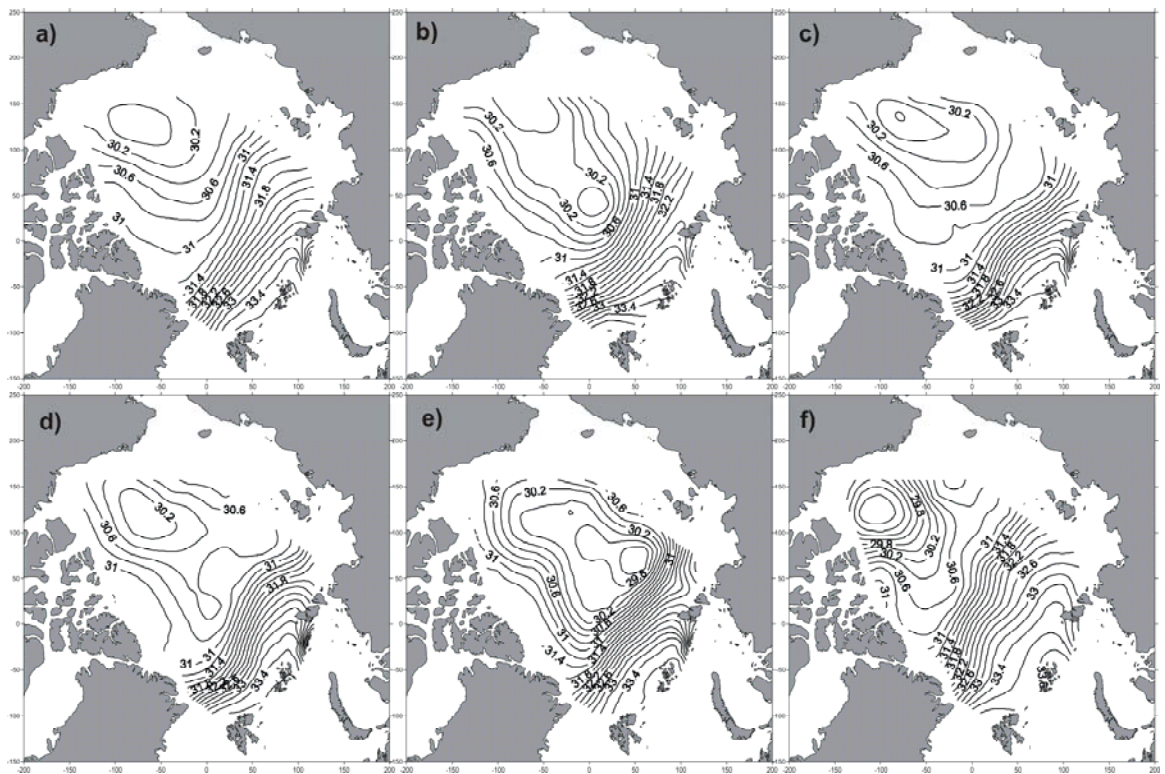
507

508 Fig. 1. Temporal changing in salinity on the depth 5-50 m (the Eurasian Basin and Canada
509 Basin) is as an example of anomalies.



510

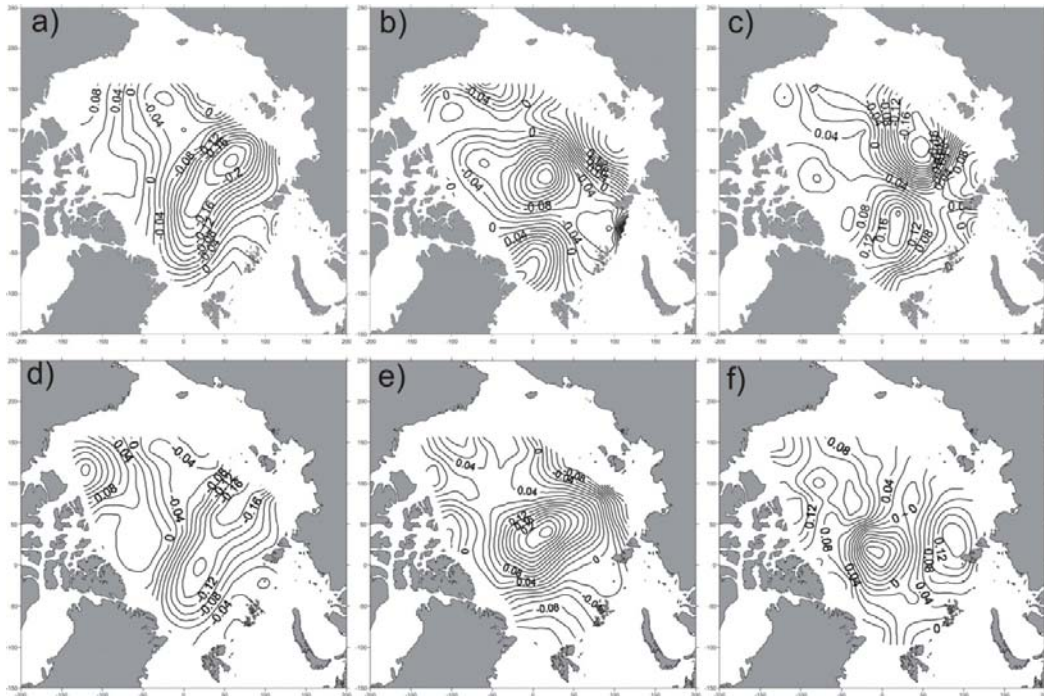
511 Fig. 2 Dendrogram of winter salinity fields for the layer 5-50 m in the Arctic basin.



512

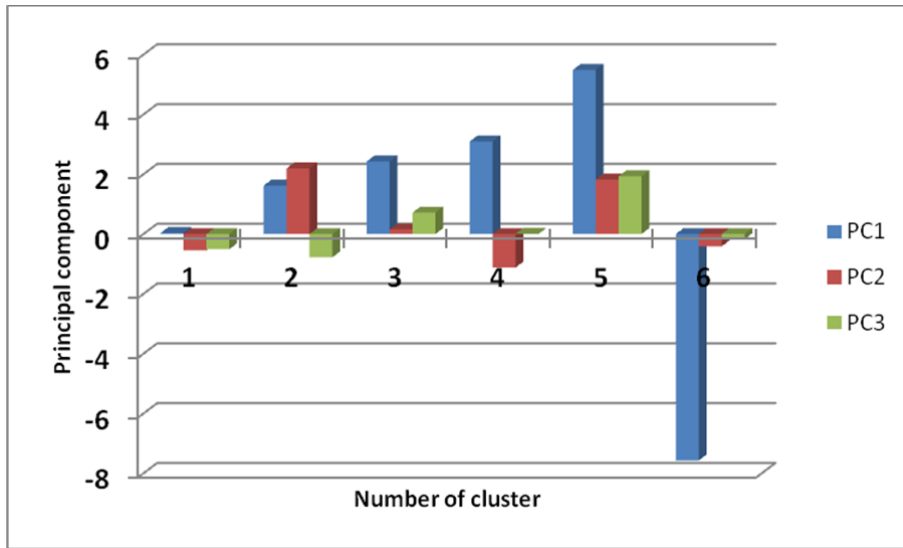
513 Fig. 3. Winter salinity fields for the layer 5-50 m averaged over periods to clusters: a – the

514 cluster 1; b – the cluster 2; c – the cluster 3; d – the cluster 4; e – the cluster 5; f – the cluster 6.



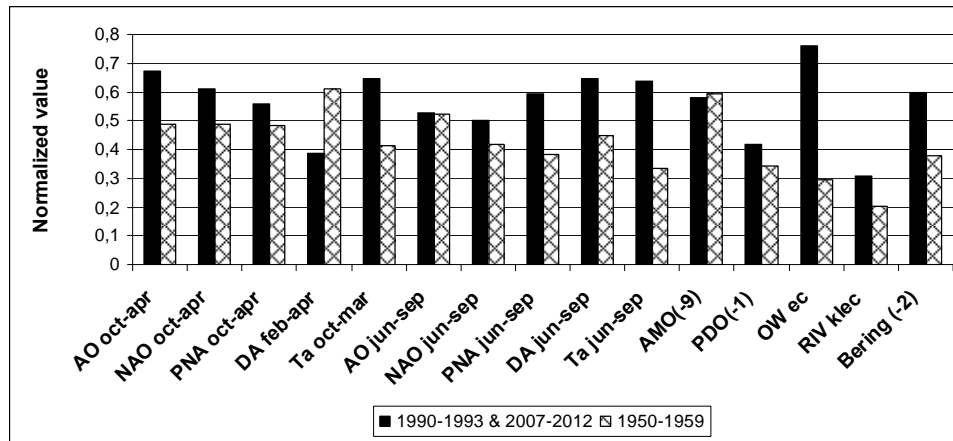
515

516 Fig. 4. The first three modes of the average salinity field decomposition for the layer 5-50 m: a,
 517 b, c - 1st, 2nd and 3rd modes, respectively, for the period 1950-1993.; d, e, f - 1st, 2nd and 3rd
 518 modes, respectively, for the period 1950-1993 and 2007-2011.



519

520 Fig. 5. The mean values of PCs for six clusters: 1 - 1950-59, 1976-77 and 1989; 2 - 1960-1965.;
 521 3 - 1966-1975; 4 - 1981-1988; 5 - 1978-1980.; 6 - 1990-93 and 2007-2012.



522

523

524

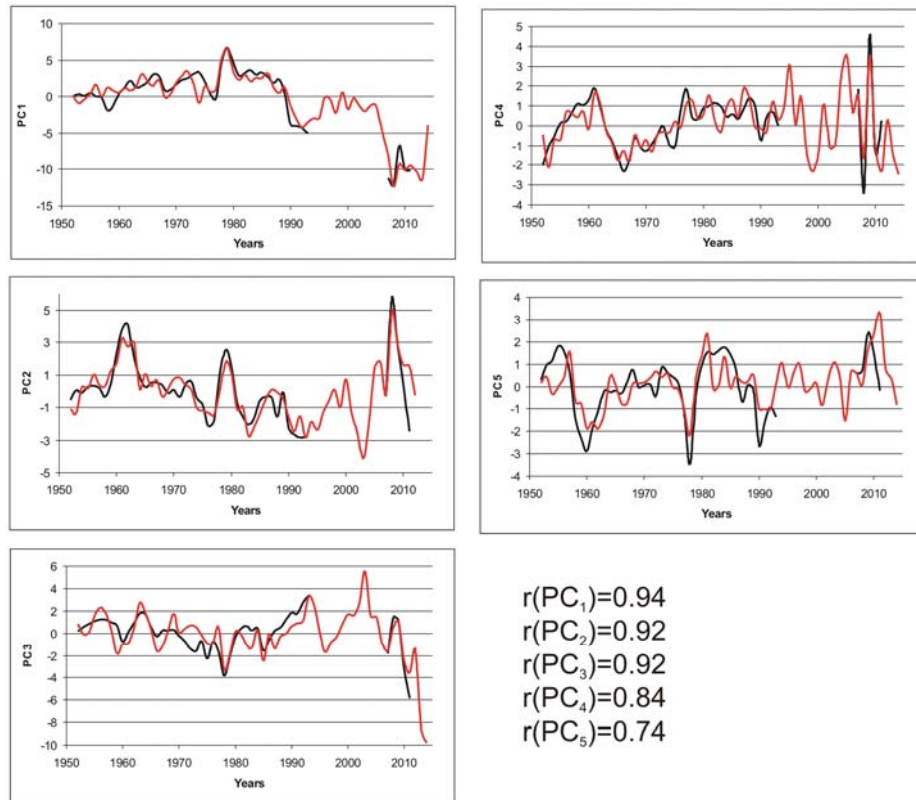
525

526

527

528

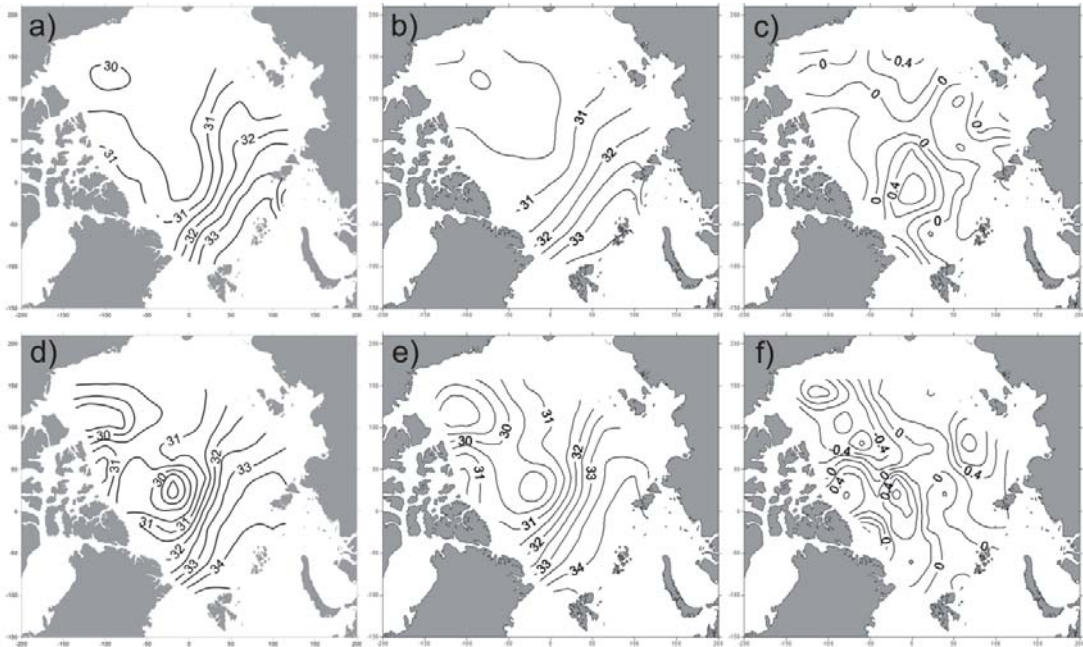
Figure 6. Mean values of the normalized values of the atmospheric circulation indexes (AO, NAO, PNA, DA, AMO, PDO); air temperature anomalies (Ta); areas of ice-free surface in the East Siberian and Chukchi Seas in September; river runoffs in the Kara, Laptev, East Siberian and Chukchi seas, the flow through the Bering Strait. Indexes of atmospheric circulation and temperature anomalies which averaged over the winter and summer months have been used in the calculations.



529

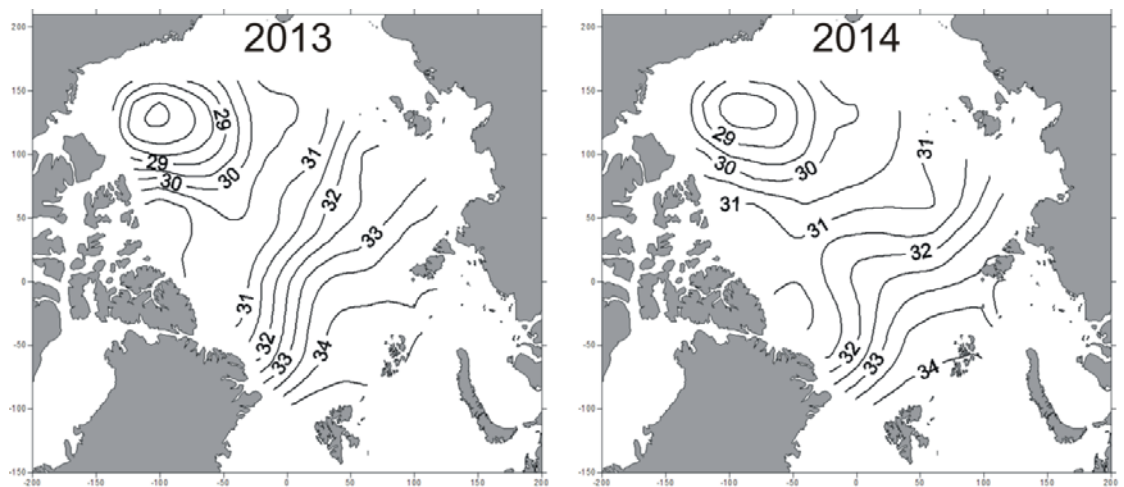
530 Figure 7. The real (black line) principal components and calculated principal components (red
531 line) with help of the equations of linear regression. Also, we show the correlation coefficients
532 between calculated time series of PC and the real PC, obtained by the decomposition of the
533 salinity fields on EOF.

534



535

536 Figure 8. The real average salinity field for the layer of 5-50 m (a, d), the reconstructed average
537 salinity field for the layer of 5-50 m (b, e) and the difference between of these fields (c, f) for
538 1955 (upper line) and 2009 (bottom line).



539
540

541 Figure 9. There is reconstructed salinity field for the layer of 5-50 m in 2013 and 2014.

543 Table 1. Predictors used for the approximation of PC.

Physical processes	Physical value	Description
Arctic oscillation index (AO)	sea-level pressure anomaly north of 20N latitude	When the AO index is positive, surface pressure is low in the polar region. When the AO index is negative, there tends to be high pressure in the polar region.
North Atlantic oscillation index (NAO)	sea-level pressure anomaly between the Icelandic low and the Azores high	When the NAO index is positive, pressures in the Azores high are especially high and pressures in the Icelandic low are lower than normal. Both pressure systems are located to the north. When the NAO index is negative, the Azores high and the Icelandic low are much weaker. Pressure differences are therefore smaller and both systems are located to the south.
Pacific/North American index (PNA)	sea-level pressure anomaly in the Northern Hemisphere extratropics	When the PNA index is positive, above-average heights over the Hawaii and over the intermountain region of North America, and below-average heights located south of the Aleutian Islands and over the southeastern United States. When the PNA index is negative, strong and extensive Hawaii high and a weak and very local Aleutian low are observed.
Arctic Dipole	sea-level	When the DA index is positive, sea-level pressure

Anomaly index (DA)	pressure anomaly north of 20N latitude	has positive anomaly over the Canadian Archipelago and negative anomaly over the Barents Sea. When the DA index is negative, SLP anomalies show an opposite scenario, with the center of negative SLP anomalies over the Nordic seas. (Wu et al, 2006; Wang et al, 2009; Overland & Wang, 2010)
Atlantic Multidecadal oscillation index (AMO)	Variations of sea surface temperature in the North Atlantic Ocean	Index has cool and warm phases that may last for 20-40 years at a time and a difference of about 0.5°C. It reflects changes of sea surface temperature in Atlantic Ocean between the equator and Greenland. Was used as substitute for processes of water exchange with Atlantic Ocean.
The Pacific Decadal Oscillation index (PDO)	North Pacific sea surface temperature variability	When the PDO index is positive, the west Pacific becomes cool and part of the eastern ocean warms. When the DA index is negative, the opposite pattern occurs. It shifts phases on at least inter-decadal time scale, usually about 20 to 30 years.
Air temperature anomaly	degree	Monthly mean anomalies of air temperature over the Arctic
river runoff	water flows	Average annual runoff of the main Siberian rivers. Was used as total runoff in Kara Sea, Laptev Sea, East-Siberian Sea and Chukchi Sea.
Ice extent	area	Total ice extent in the Arctic Ocean in September

Area of open water in Arctic seas (OW)	area	Total ice-free area in Kara Sea, Laptev Sea, East-Siberian Sea and Chukchi Sea in September
Bering Strait inflow (BS)	water flows	Average annual water exchange through the Bering Strait

544

545

546

547

548

549

550